

Optimization-based Thermal Control Strategy for Auxiliary Cooling Circuits in Fuel Cell Vehicles

Yousif Eldigair, Cristian Kunusch, *Senior Member, IEEE*, and Carlos Ocampo-Martinez, *Senior Member, IEEE*

Abstract—In this research work, a thermal management concept for the auxiliary components in fuel cell vehicles is discussed. A control-oriented model of the subsystem under analysis is developed and then used as basis for controller development. Two control strategies are implemented and compared. The first is a PI-controller strategy and it is used as a baseline for performance comparison. The second is an optimization-based controller (OBC) strategy focused on minimizing the power consumption of the main actuator. The OBC features a novel steady-state observer (SSO) developed for thermal circuits and provides an estimation of the steady-state conditions and conveniently simplifies the optimization problem by disregarding the dynamics of the states so that it can be implemented online with lower computational burden. Comparisons between PI-control strategy and OBC demonstrate the OBC's capabilities in overcoming typical problems associated with the PI-control strategy including high power consumption of the actuators and temperature constraint violations under particular operating conditions.

Index Terms—thermal management, fuel cells

I. INTRODUCTION

OUT of all known types of fuel cell systems, the proton exchange membrane fuel cell systems (PEMFC) is seen to have the most potential in the automotive industry [1]. This is primarily due to the fact that PEMFC systems are able to operate at relatively lower temperature (30°C to 100°C) compared to other fuel cell systems, while having a sufficiently high power density. Automotive PEMFC systems, under optimal operating conditions, are generally associated with efficiencies close to 50% [2]. The inefficiencies are predominantly reflected as heat, whether it be the heat generated in the stack or in the auxiliaries of the system. If the temperature of the fuel cell stack is allowed to rise significantly beyond its nominal operating temperature, it could result in the dehydration in the membrane layer which ultimately leads to an irreversible performance loss [3]–[5]. Therefore, to ensure that the integrity of the fuel cell system is not compromised due to high temperatures variations, a thermal management subsystem is heavily relied on to provide sufficient cooling during operation or heating during cold start-up. This also applies to the auxiliaries of the fuel cell system.

Most of the studies related to the thermal management of PEMFC systems discuss the modeling and control of a single

coolant loop in which the PEM stack is cooled without much consideration of the auxiliaries of a typical fuel cell vehicle [6]–[8]. These auxiliaries include the fuel cell compressor's motor and power electronics, the DC-DC converter which connects the stack to the high voltage bus and also an air intercooler. The prime function of the air intercooler is to cool down the compressed air which flows into the stack's cathode. If the compressed air, which can reach temperatures beyond 100°C depending on the operating conditions, is allowed to flow into the fuel cell stack without cooling, it may result in irreversible damage by melting the membrane layer. Furthermore, proper regulation of the air temperature contributes to higher efficiencies and extends the life span of the stack [9]. Since liquid-gas intercoolers offer better cooling than gas-gas intercoolers due to the higher heat capacity of the liquid coolant, they are more compact and hence are more suitable for vehicular integration.

Some studies do consider the modeling and control of the crucial auxiliary components [7], [10], [11]. PI-based control strategies have been used for the control of the cooling circuits to ensure coolant temperature references are tracked. In the 2015 Toyota Mirai, the cooling subsystem associated with the PEMFC system is comprised of a single coolant circuit in which coolant is pumped through both the stack and a liquid-gas intercooler [12]. Other more detailed topologies of vehicle integrated thermal management (VITM) systems in fuel cell electric vehicles can be shown [13]–[16]. Both the fuel cell stack and the battery operate at different optimal temperatures, whereas other system auxiliaries, such as motors or power converters only require only that the cooling be sufficient. For this reason, VITM systems are typically composed of different cooling loops, each operating at different temperatures [13]–[15].

In the scheme of vehicular energy management, optimization-based control strategies have provided a good framework for reducing the energy consumption and enhance the efficiency of the overall vehicle [17]. When applied to the drive train of hybrid electric vehicles, optimization-based controllers (OBCs), whether done offline (such as in [18], [19]) or online (such as in [20]), have been proved effective. In [21], an OBC in the frame of nonlinear model predictive control (MPC) was proposed for one of three cooling loops of the thermal management system of a plug-in hybrid electric vehicle. The thermal loads considered in the cooling loop were the battery bank and its associated power electronics. The OBC implemented lead to improvement in terms of energy consumption while fulfilling all the requirements of the vehicle integrated thermal management (VITM) system.

Yousif Elidgair is with Brose Fahrzeugteile SE & Co. Kommanditgesellschaft, Würzburg, Germany. (e-mail: yousif.eldigair@brose.com).

Yousif Elidgair and Carlos Ocampo-Martinez are with the Institut de Robòtica i Informàtica Industrial, Universitat Politècnica de Catalunya, CSIC-UPC, Barcelona, Spain.

Cristian Kunusch is with Valeo Siemens eAutomotive Germany GmbH, Erlangen, Germany.

Nonetheless, the OBCs required knowledge of the nonlinear system dynamics associated with all components. This naturally lead to a more complex optimization problem. Some of the dynamics of the thermal elements could also be difficult to predict under different driving or ambient conditions.

In this paper, the modeling and control of a fuel cell auxiliary cooling circuit (FCAC) of a fuel cell electric vehicle is discussed. The FCAC has been developed to cool the auxiliaries of the fuel cell system but not the fuel cell stack itself. The fuel cell stack requires another cooling circuit operating at higher temperature and is out of the scope of this paper. FCACs are a necessary must in fuel cell electric vehicles. The main objective of FCACs is to provide key components, such as air compressors and power converters, with sufficient cooling under high load to avoid overheating. To do so, they are controlled in such a fashion to keep the coolant temperatures at the inlet of auxiliary components below certain limits.

The main contribution of this paper resides in the new OBC design approach and implementation on FCACs. The control-oriented model (COM), used for optimization, was made based on a novel steady-state observer (SSO) which estimates the states and outputs of the FCAC at steady state without requiring knowledge of the dynamic behavior of the system. The COM innovatively disregards all dynamics seen with the states $x(t)$ and just looks at $x(t)$ at steady state ($t \rightarrow \infty$). No knowledge of the current states is needed; rather, only the control inputs u and other parameters are required. This reduction/simplification applied to thermal management systems is a point of contribution of this paper and conveniently simplifies the optimization problem making it easier to implement online. It can be seen that the developed OBC is effectively able to minimize the power consumption of the cooling circuit while abiding by all the temperature and mass flow constraints. FCACs are a particularly suitable application to the developed OBC, since the dynamics of the thermal systems are slow (convergence times greater than 50s) and are not of huge importance.

The structure for the remainder of the paper is organized as follows: Section II gives an overview of the FCAC, describing the functions of the components included within the loop. It also goes through the dynamic modeling of the FCAC building up to a simulation-oriented model (SOM). Finally in Section II, the control objectives are presented. In Section III-A, a PI-control strategy for control of the FCAC is implemented using typical PI-control. Section III-B provides the general structure of the OBC and then proceeds in developing a SSO based on a static COM. Thereafter, the optimization problem is formulated and simulation results of the OBC are presented. In Section IV, comparisons between the PI-control strategy and OBC are made, highlighting the differences between both approaches. Section V proposes a methodology based on the developed SSO to simplify the structure of the OBC such that it can be implemented on an automotive microcontroller. Finally, conclusions for this paper are drawn in Section VI.

II. SYSTEM DESCRIPTION

In an automotive fuel cell system, air is driven through the cathode line by using an electric compressor. Under high mass flow rates and pressures, the air exhibits a temperature rise from compressor inlet to outlet. The speed of rotation of the compressor, mass flow rate of air, pressure ratio from inlet to outlet and temperature of the air at the outlet are related. The relations can best be described through static performance maps.

To cool the air after compression, an intercooler is generally incorporated downstream of the compressor to cool down air to acceptable levels. Furthermore, due to unavoidable electrical and mechanical losses, in the compressor and its converter, both the motor and power electronics of the compressor require cooling under continuous operation. In addition to the inverter used for the compressor, a DC-DC converter is required to connect the fuel cell stack to the high voltage bus bar. This converter also requires cooling due to the heat generated due to switching losses. While this varies based on loading conditions, the combined efficiency of the compressor's drive and motor is around 90% and the efficiency of the DC-DC converter is around 98%. Moreover, the compressor can generate air mass flow rates of up to 120 g/s at temperatures of upto 160°C which needs to be cooled to around 70°C. Taking that into consideration, a FCAC is needed to dissipate heat and cool the air after compression.

A. System Layout

A schematic of the FCAC is presented in Fig. 1. As it can be seen, the system is comprised of a radiator with a cooling fan, an expansion tank, and electric turbo-compressor with its inverter, a DC-DC converter, a liquid-gas intercooler, a centrifugal pump and two three-way diverter valves. Based on the operating conditions, the radiator has been designed to have a cooling capacity of 9kW under nominal operation. This would be sufficient to provide adequate cooling to the system.

B. System Model

1) *Thermodynamics*: By analyzing the in-flow and out-flow of enthalpy h and the heat flow \dot{Q} , the dynamics of the thermal elements within the FCAC can be modeled. As dictated by the first law of thermodynamics [22],

$$\frac{d}{dt}(mu) = h_{in}W_{in} - h_{out}W_{out} \pm \dot{Q}, \quad (1a)$$

$$\frac{dm}{dt} = W_{in} - W_{out}. \quad (1b)$$

In (1b), u denotes the specific internal energy (in J/kg) within the particular volume, m is the mass (in kg) of fluid within the volume, h_{in} and h_{out} denote the specific enthalpy (in J/kg) flowing into and out of a particular volume, W_{in} and W_{out} are the mass inflow and outflow rates (in kg/s) respectively, \dot{Q} denotes the heat flow rate (in W) from the volume with hot medium to volume with cold medium. It should be noted that W_{in} can be assumed W_{out} at steady state. Depending on whether the medium gains or losses heat, either $+\dot{Q}$ is used or $-\dot{Q}$.

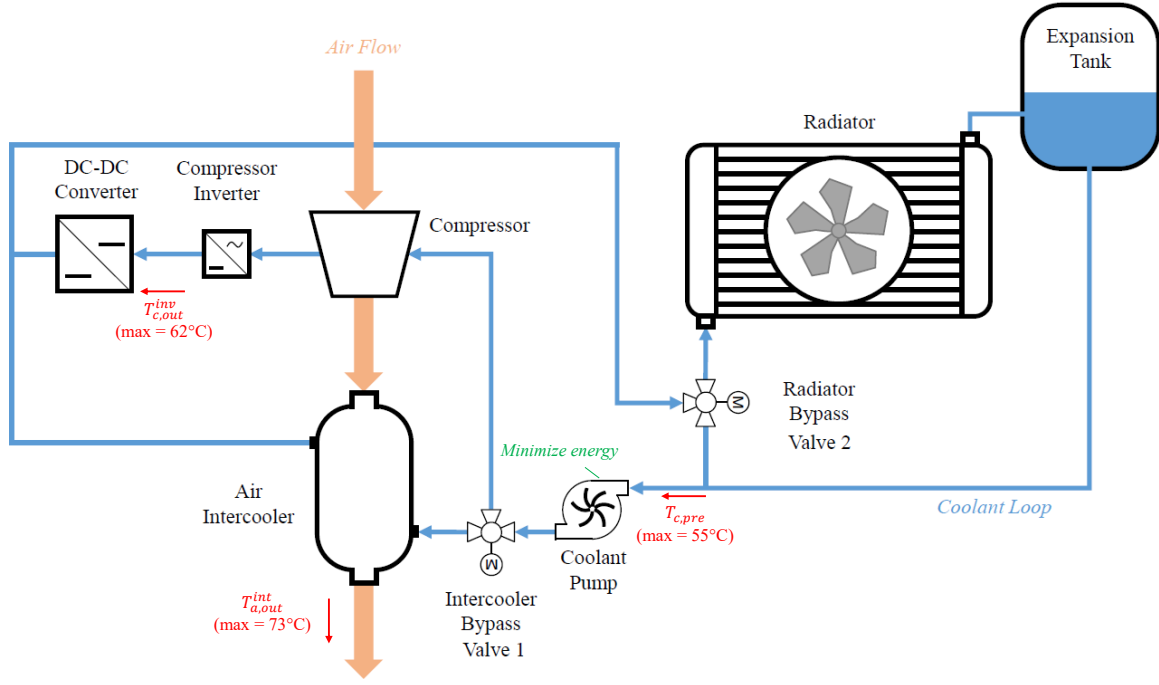


Fig. 1. Fuel cell auxiliaries cooling circuit (FCAC)

The internal energy u within a volume and the enthalpy h flowing into or out of the volume varies with the temperature T (in K) and can be expressed as [22]

$$u = \int C_v dT, \quad (2a)$$

$$h = \int C_p dT, \quad (2b)$$

where T is the temperature, C_v and C_p are the specific heat capacity under constant volume and pressure respectively. The relation of u and h with T for various materials can be expressed in maps.

2) *Heat Exchangers*: Within the FCAC system, there are two heat exchangers that transfer heat from one medium to another. As depicted Fig. 1, one is a radiator and the other is the air intercooler. There are essentially two volumes in a heat exchanger through which the cold and hot mediums flow. It should be stated that in the radiator, the hot medium is the coolant and the cold medium is the air passing through the radiator fins. A heat flow rate \dot{Q}_{rad} from the coolant to the air can be defined for the radiator. As for the intercooler, the heat flow rate \dot{Q}_{int} is defined from the coolant to the air. Modeling of heat exchangers can be done using (2a). For both heat exchangers, the heat flow rate depends on the temperature differential between the hot and cold media can be found through

$$\dot{Q} = (T_{hot} - T_{cold})\alpha, \quad (3)$$

where α is the heat transfer coefficient (in W/K). Generally, α is influenced by design parameters such as the cross-sectional area between the two volumes and the wall material and thickness. In order to develop a control-oriented model, it is convenient to make use of lookup tables that include experimental data where α can be obtained for given mass flow

rates and temperatures. Moreover in (3), T_{hot} and T_{cold} are the average temperatures in the hot and cold volumes respectively. Accordingly, the average coolant temperature in the radiator $T_c^{rad} = T_{hot}$ and the air temperature $T_a^{rad} = T_{cold}$. As for the intercooler, $T_c^{int} = T_{cold}$ and $T_a^{int} = T_{hot}$. It should be noted that “ a ” subscript is used to refer to air and “ c ” subscript is used for the coolant. Assuming that the change in temperature occurs linearly from the inlet to the outlet of the volumes, the following hold:

$$T_{hot} = \frac{T_{in}^{hot} + T_{out}^{hot}}{2}, \quad (4a)$$

$$T_{cold} = \frac{T_{in}^{cold} + T_{out}^{cold}}{2}. \quad (4b)$$

3) *Air Compressor and Power Inverter*: The heat flow rates \dot{Q}_m and \dot{Q}_{inv} produced by the compressor’s motor and its inverter are influenced by the operating conditions; as in the mass flow rate of air through the compressor, which is equivalent to $W_{a,in}^{int}$, and the pressure ratio PR from inlet to outlet of the compressor. The experimental results were used to create static maps that can be used to obtain the \dot{Q}_m and \dot{Q}_{inv} from $W_{a,in}^{int}$ and PR . Generally, $W_{a,in}^{int}$ is usually controlled based on the fuel cell stack current demand, in order to regulate the oxygen stoichiometry and improve the system efficiency. This is also crucial in order to avoid irreversible damage due to oxygen starvation in the stack.

Based on the stack power output P_{stk} , a certain oxygen stoichiometry (obtained through manipulating $W_{a,in}^{int}$) and operation pressure (which translates to a specific PR) would lead to optimal operation of the overall fuel cell system in terms of efficiency. However, since the electrical and air flow dynamics associated with the stack and the cathode line are considerably faster than the thermal dynamics associated with

the FCAC, the detailed model of the stack can be replaced by a static map. For a stack power output P_{stk} , the map would yield $W_{a,in}^{int}$ and PR required for optimal operation. The power profile from a typical driving cycle along with this map can then be used to obtain profiles for $W_{a,in}^{int}$ and PR and test the performance of the FCAC.

Based on the output voltage and current of the fuel cell stack, the DC-DC converter produces a heat at a rate \dot{Q}_{dc} . A static map is used to approximate \dot{Q}_{dc} based on the power demand of the vehicle's drive train P_{veh} . Knowing \dot{Q}_m , \dot{Q}_{inv} and \dot{Q}_{dc} , (2a) can be used to model the temperature rises in the coolant as it flows through the thermal components.

4) *Radiator Air Flow*: The mass flow of air through the radiator is required to calculate the heat transfer coefficient α_{rad} in order to model the cooling done by the radiator. The car manufacturer provided data based on fluid analysis simulations. The data relates the mass flow rate of air through the radiator to the speed of the vehicle and the control action of the cooling fan.

Given (1b)-(4b), a SOM was developed in a Matlab/Simulink environment. This was used to test the control strategies later discussed in this paper.

C. Control Objectives

The control of the FCAC must be done to achieve three main objectives and also two secondary objectives under varying ambient conditions of temperature and pressure and also in the presence of disturbances. There are different external disturbances that affect the FCAC subsystem. One of them is the airflow through the radiator fins due to changes in v_{car} and u_{fan} . It should be emphasized here that the cooling fan is not to be controlled by the FCAC; rather, it is an actuator of another cooling subsystem (high temperature circuit) that is out of the scope of this paper. That considered, the controllers developed and presented later on in this paper consider cooling fan only an external disturbance. This is also true for the electric compressor, which is controlled by another subsystem to ensure that the required mass flow rate is supplied to the stack such that it is not starved of the oxygen it needs to produce electric current. The compressor also introduces disturbances to the FCAC through the temperature, flow rate and pressure of the air flowing into the intercooler. Furthermore, the motor and electronics of the compressor, as well as the DC-DC converter are heat sources that depend on the operating conditions of the fuel cell system. This fact must be considered when constructing a model of the FCAC subsystem.

During the development phase of the fuel cell stack, different thermal simulations were made and a testing campaign was done. The simulations and testing concluded that 73°C as a maximum value for the air temperature entering the stack, provides a suitable safety margin to avoid irreversible damages to the fuel cell membranes due to high temperature. Similarly, thermal testing of the electric compressor also showed that coolant flowing into the motor's cooling jacket with temperatures exceeding 55°C lead to the formation of hot spots in the stator which leads to motor damage. Furthermore, the provider of the DC-DC converter reported that coolant temperatures

above 62°C would provide insufficient heat dissipation at high fuel cell currents. Using the information provided, the three primary objectives are henceforth defined and must be satisfied to avoid damage to the system. These are the following:

- 1) **The air temperature $T_{a,out}^{int}$ at the outlet of the intercooler must be below 73°C .**

Since this is the air that flows into the cathode of the stack, higher temperatures pose risk of damage to the stack of the membrane. During the development phase of the fuel cell stack, simulations using a thermal model were done. These simulations concluded that an air temperature of 73°C provides a safety margin such that damage to the membrane in the stack due to high temperature is avoided even during peak stack output power.

- 2) **The coolant temperature before cooling $T_{c,pre}$ must be lower than 55°C .**

One of the aspects tested during the compressor commissioning was the cooling requirements, particularly for the electric motor. It was found that when the temperature of the coolant exceeded 55°C , hot spots started to form. As a result, the compressor cannot fully operate and achieve all desired mass flow rates and must be de-rated. This condition in turn limits the operation of the fuel cell system and therefore must be avoided.

- 3) **The coolant temperature $T_{c,out}^{inv}$ at the outlet of the compressor's inverter must be lower than 62°C .**

It was reported that temperatures below 62°C would provide inadequate cooling for the DC-DC converter and would lead to the accumulation of heat and overtime would cause the overheating of the power electronics, particularly at high power outputs from the fuel cell stack.

The secondary objectives are set to enhance the efficiency of the overall FCAC system and are the following:

- 1) **The air temperature $T_{a,out}^{int}$ should preferably be as close to the optimal temperature of 73°C as possible.**

Lower air temperatures reduce the efficiency of the stack and higher temperatures pose a risk of damage to the membrane.

- 2) **The pump control u_{pmp} should preferably be low.**
This is to reduce the power consumption of the FCAC system.

It is noteworthy that, for such a thermal system, it is the steady state which is of interest; specifically, the constraints (whether satisfied or not), the steady-state error for $T_{a,out}^{int}$ and finally, the power consumption of the cooling pump. As long as there are no significant high temperature overshoots, the dynamics associated with the closed-loop response are of little interest.

To achieve the aforementioned control objectives, three actuators are available; namely, the two three-way valves and the coolant pump. These actuators are manipulated through u_{v1}^* , u_{v2}^* and u_{pmp}^* and dictate the flow rates through the

TABLE I
SIMULATION TEST SCENARIOS

	T_{amb} (C°)	W_{cp} (g/s)	PR (-)	v_{car} (km/h)
Scenario 1	-10	80	1.8	30
Scenario 2	35	55	1.4	60
Scenario 3	-10	120	2.2	115

components as follows:

$$W_{c,rad} = W_{pmp}^{\max} u_{pmp} u_{v2}, \quad (5a)$$

$$W_{c,m} = W_{pmp}^{\max} u_{pmp} u_{v1}, \quad (5b)$$

$$W_{c,int} = W_{pmp}^{\max} u_{pmp} (1 - u_{v1}), \quad (5c)$$

where W_{pmp}^{\max} is the maximum coolant flow rate which can be delivered by the cooling pump. At maximum speed, the pump consumes 1 kW of electric power which is the main parasitic loss of the auxiliary cooling loop.

The control should be implemented in such a way to be able to successfully fulfill the aforementioned objectives under various operating conditions. In this paper, three different scenarios of ambient temperature T_{amb} , pressure ratio PR from inlet to outlet of the compressor, mass flows W_{cp} at outlet of the compressor and car speeds v_{car} have been selected and used to evaluate the performances of the controllers developed. These test scenarios are summarized in Table. I.

It should be emphasized that, for all forthcoming simulations, the model is started at ambient conditions, the temperatures and pressures of the air and coolant in all volumes equal to the ambient pressure and temperature. The parameters W_{cp} , PR and v_{car} are then changed simultaneously in a step fashion. This extreme case of having step changes, while not fully representative of what occurs in a typical driving cycle, is enough to illustrate the closed-loop dynamic behavior of the system and controller. However, the dynamic behavior is not significant in the FCAC. The controller performance is evaluated based not on the dynamic behavior; rather, on the steady-state and its ability to fulfill the aforementioned control objectives.

III. CONTROLLER DESIGN

A. PI Control

PI-controllers are widely adopted as a solution in most industrial applications. This is also the case for the automotive industry. Their success can be justified by their effectiveness in control feedback loops without internal restrictions and their simple structure, making them suitable for implementation on rudimentary automotive microcontrollers. Furthermore, tuning of PI-controllers requires adjusting just two control parameters (K_p and K_i) and can be done manually without detailed knowledge of the system model.

To satisfy the aforementioned control objectives, three PI-controllers were used, each generating a control signal for each

of the actuators. The PI-control strategy can be expressed as

$$\begin{aligned} u_{pmp} &= K_{p1}(T_{a,out}^{int} - T_{a,out}^{int*}) + K_{i1} \int (T_{a,out}^{int} - T_{a,out}^{int*}) dt, \\ u_{v1} &= K_{p2}(T_{c,in}^{dc} - T_{c,in}^{dc*}) + K_{i2} \int (T_{c,in}^{dc} - T_{c,in}^{dc*}) dt, \\ u_{v2} &= K_{p3}(T_{c,pre}^* - T_{c,pre}) + K_{i3} \int (T_{c,pre}^{max} - T_{c,pre}) dt. \end{aligned} \quad (6)$$

where the setpoint $T_{a,out}^{int*}$ is the air temperature setpoint after the intercooler and is 73°C. This is to be controlled through the pump via u_{pmp} which manipulates the mass flow of the coolant; thus, the heat flow rate \dot{Q}_{int} and the temperature $T_{a,out}^{int}$. The setpoint $T_{c,in}^{dc*}$ is for the temperature of the coolant flowing into the DC-DC converter and is set to 62°C as not to exceed the converter limit of 60°C. This is tracked by using valve V-1. By increasing the mass flow $W_{c,dc}$ through the compressor and its inverter, i.e., increasing u_{v1} , the temperature rises across these two components is reduced, which in turns reduces $T_{c,in}^{dc}$. Finally, the setpoint $T_{c,pre}^*$ is for the coolant temperature pre-cooling (location is shown in Fig. 1). When $u_{v2} = 1$, all the coolant flow is passed through the radiator leading to more cooling and a lower $T_{c,pre}$. A setpoint of $T_{c,pre}^* = 50°C$ is used to add a safety margin of 5°C as not to exceed the 55°C limit of the coolant flowing into the compressor.

There are systematic tuning methods for selecting the K_p and K_i parameters of the PI-controllers. Tuning in this case was performed to achieve a settling time less than 100s and avoid overshoots in the coolant temperatures greater than 10%.

B. Optimization-Based Controller (OBC)

The control of the FCAC naturally manifests as an optimization problem, where the control of the coolant temperature into the compressor's motor and DC-DC converter are reflected as constraints to an associated optimization problem. Furthermore, it is desirable to have the minimum power consumption of the FCAC through having the pump operate with the least amount of coolant flow while still fulfilling the primary control objectives given in Section II-C. This information was used to develop an OBC which runs online to yield the control signals for the three actuators.

1) *Steady-state Observer (SSO)*: The OBC is based on a simplified COM of the FCAC. A distinction is to be made between the simulation-oriented model (SOM) and the simplified control-oriented model (COM). The COM is static and disregards the dynamics associated with the system states. Rather, the COM is based on a SSO which computes the system states and outputs at steady-state operation for a particular set of control inputs. Furthermore, some of the equations that are outlined in Section II-B and used to develop the SOM were simplified for use in the SSO. It should be noted that, in order to simplify the optimization problem associated with the OBC, the SSO assumes that successful control of $T_{a,out}^{int}$ is achieved at steady state. To correct any inaccuracies that stem from the simplifications, feedback from the SOM from readily available sensors is used. This ultimately provides an estimation of the system at steady state.

One simplification that is applied within the COM is the method by which the specific heats C_p and enthalpies h are evaluated for the coolant and air. While they are evaluated using lookup tables in the SOM, linear regression can be done to express these maps as follows:

$$C_{p,k} = a_{0,k} + a_{1,k}T_k, \quad (7)$$

$$T_k = b_{0,k} + b_{1,k}h_k, \quad (8)$$

where $a_{0,k}$, $a_{1,k}$, $b_{0,k}$ and $b_{1,k}$ are regression coefficients and the k notation signifies the medium (air or coolant).

When considering the steady state of components in the thermal circuit, it can be assumed that for all components, $W_{in} = W_{out} = W$. Therefore, the temperature rises from inlet to outlet can be modeled as

$$\dot{Q} = (T_{in}C_{p,in} \pm T_{out}C_{p,out})W. \quad (9)$$

Using (9), the dynamics of temperature are neglected. This can be used for all heating elements making the model simple and suitable for an OBC. Furthermore, during steady-state operation, the net heat transfer \dot{Q}_{total} should be 0. Accordingly,

$$\dot{Q}_{int} + \dot{Q}_m + \dot{Q}_{inv} + \dot{Q}_{dc} - \dot{Q}_{rad} - \dot{Q}_{tnk} = 0, \quad (10)$$

where the subscripts int , m , inv , dc , rad and tnk denote the intercooler, compressor's motor, compressor's inverter, DC-DC converter, radiator and tank respectively. \dot{Q}_{tnk} can be considered null since it is typically very small with respect to the other thermal elements in the cooling loop. Similar to the SOM, \dot{Q}_{rad} and \dot{Q}_{int} in the COM are evaluated using (3) where α_{rad} and α_{int} are obtained using lookup tables.

Under successful control of $T_{a,out}^{int}$, where $T_{a,out}^{int} = T_{a,out}^{int*}$, the heat flow rate of the intercooler, which would be the feed-forward \dot{Q}_{int}^{FF} , can be evaluated using

$$\dot{Q}_{int}^{FF} = (T_{a,in}^{int}C_{p,in} - T_{a,out}^{int*}C_{p,out})W_{a,int}. \quad (11)$$

It should be noted that when $T_{a,in}^{int} \leq T_{a,out}^{int*}$, the intercooler is bypassed from the coolant side by having $u_{v1} = 1$. This in turn leads to a $\dot{Q}_{int}^{FF} = 0$ and accordingly $T_{a,out}^{FF} = T_{a,in}^{int}$. Using (9)-(10), the feed-forward radiator heat flow rate can be evaluated as

$$\dot{Q}_{rad}^{FF} = \dot{Q}_{int}^{FF} + \dot{Q}_m + \dot{Q}_{inv} + \dot{Q}_{dc}. \quad (12)$$

Given $T_{a,in}^{rad}$, $W_{a,rad}$ and \dot{Q}_{rad}^{FF} under successful control, the temperature of air after the radiator can be found through

$$\hat{h}_{a,out}^{rad} = T_{a,in}^{rad}C_{p,a,in} + \frac{\dot{Q}_{rad}^{FF}}{W_{a,rad}}, \quad (13)$$

Notation \hat{x} denotes that the variable is an estimate of x where x is general term and can represent temperature, specific heat, enthalpy, heat flow rate or heat transfer coefficient. Using (8), $\hat{T}_{a,out}^{rad}$ can be calculated. Knowing $W_{c,rad}$ from the control inputs u_{pmp} and u_{v2} , the heat transfer coefficient $\hat{\alpha}_{rad}$ of the radiator can be obtained through the lookup table. Having obtained $\hat{T}_{a,out}^{rad}$ from (13), the outlet coolant temperature of the radiator can be obtained through

$$\hat{T}_{c,out}^{rad} = \hat{T}_{a,out}^{rad} + \frac{\dot{Q}_{rad}^{FF}}{\hat{\alpha}_{rad}}. \quad (14)$$

This would be the required outlet coolant temperature needed to sustain a steady state where $T_{a,out}^{int}$ is successfully controlled. From $\hat{T}_{c,out}^{rad}$, the radiator inlet coolant enthalpy $\hat{h}_{c,in}^{rad}$, therefore temperature $\hat{T}_{c,in}^{rad}$, can be found as follows:

$$\hat{h}_{c,in}^{rad} = \hat{h}_{c,out}^{rad} + \frac{\dot{Q}_{rad}^{FF}}{W_{c,rad}}. \quad (15)$$

With $\hat{T}_{c,in}^{rad}$ and $\hat{T}_{c,out}^{rad}$ known, the pre-heating coolant enthalpy $\hat{h}_{c,pre}$, and therefore $\hat{T}_{c,pre}$ can be evaluated as follows:

$$\hat{h}_{c,pre} = \hat{C}_{p,in}\hat{T}_{c,in}^{rad}(1 - u_{v2}) + \hat{C}_{p,out}\hat{T}_{c,out}^{rad}u_{v2}. \quad (16)$$

Under nominal conditions, if there are no mismatches between the SOM and COM, $\hat{T}_{c,pre} = T_{c,pre}$ at steady state. However, due to the mismatches, a correction must be done based on the estimation error $e_1 = T_{c,pre} - \hat{T}_{c,pre}$. This correction is reflected on the COM as a fictitious source given by \dot{Q}_{corr} which is evaluated as

$$\dot{Q}_{corr} = K_{p1}^{SSO}e_1 + K_{i1}^{SSO} \int e_1 dt, \quad (17a)$$

$$\hat{h}_{c,pre}^{corr} = \hat{T}_{c,pre}\hat{C}_{p,pre} + \frac{\dot{Q}_{corr}}{W_{pmp}}, \quad (17b)$$

$$\hat{T}_{c,pre}^{corr} = h_{c0} + h_{c1}\hat{h}_{c,pre}^{corr}, \quad (17c)$$

where K_{p1}^{SSO} and K_{i1}^{SSO} are positive constants that determine the error convergence dynamics and $\hat{T}_{c,pre}^{corr}$ is the corrected pre-cooling coolant temperature and should eventually converge to the actual $T_{c,pre}$.

Given $\hat{T}_{c,pre}^{corr}$ and $W_{c,dc}$ from u_{pmp} and u_{v1} and knowing the heat flow rates \dot{Q}_m , \dot{Q}_{inv} and \dot{Q}_{dc} , the temperatures $\hat{T}_{c,out}^m$, $\hat{T}_{c,out}^{inv}$ and $\hat{T}_{c,out}^{dc}$ can then be evaluated similar to (15). Knowing $W_{c,int}$ from u_{pmp} and u_{v1} and having $T_{a,in}^{int}$ and $W_{a,in}^{int}$ as inputs to the SSO, $\hat{\alpha}_{int}$ can be obtained which should be equal to α_{int} . However, due to model discrepancies, it is to be expected that the value of $\hat{\alpha}_{int}$ of the SSO will be different from that of the actual hardware; thus, leading to different values of \dot{Q}_{int} and $T_{a,out}^{int}$. A correction based on the error $e_2 = T_{a,out}^{int} - \hat{T}_{a,out}^{inv}$ is therefore incorporated through

$$\tilde{\alpha}_{int} = K_{p2}^{SSO}e_2 + K_{i2}^{SSO} \int e_2 dt, \quad (18)$$

$$\alpha_{int}^{corr} = \hat{\alpha}_{int} + \tilde{\alpha}_{int}, \quad (19)$$

where K_{p2}^{SSO} and K_{i2}^{SSO} are positive constants. Finally, to calculate $\hat{T}_{a,out}^{int}$, α_{int}^{corr} is first used to evaluate \dot{Q}_{int} as follows:

$$\dot{Q}_{int} = \frac{\frac{\hat{C}_{p,a,in}^{int}T_{a,in}^{int}}{C_{p,a,out}^{FF}} - \frac{\hat{C}_{p,c,in}^{int}T_{c,pre}^{corr}}{C_{p,c,out}^{FF}}}{\frac{1}{\alpha_{int}^{corr}} + \frac{1}{W_{c,int}C_{p,c,out}^{FF}} + \frac{1}{W_{a,int}C_{p,a,out}^{FF}}}, \quad (20)$$

$$\hat{h}_{a,out}^{int} = C_{p,a,in}^{int}T_{a,in}^{int} - \frac{\dot{Q}_{int}}{W_{a,int}}, \quad (21)$$

$$\hat{T}_{a,out}^{int} = h_{c0} + h_{c1}\hat{h}_{a,out}^{int}. \quad (22)$$

It should be noted that (20) requires the specific heats of the air and coolant at the outlet. The problem can be simplified by considering the values under the assumption that air temperature control is achieved and $\dot{Q}_{int} = \dot{Q}_{int}^{FF}$. While this simplifies the evaluation, it introduces minor inaccuracies. The inaccuracies are, however, corrected by α_{int} .

2) *Optimization Problem*: The OBC is structured around an optimization problem. The problem is primarily the minimization of the error $e_T = T_{a,out}^* - \hat{T}_{a,out}^{int}$. Note that there is a set of solutions (u_{pmp} , u_{v1} and u_{v2}) to minimize e_T , some of which violate the coolant temperature constraints and some are more desirable than others since they can reduce the energy consumption of the pump. While the PI-control strategy does not take account of the constraint problem associated with the states, the OBC can be attuned through its optimization problem to specifically target the solutions which minimize e_T , do not violate the constraints while also using the least amount of energy to run the coolant pump.

The optimization problem considered by the OBC is stated as follows:

$$\begin{aligned} \min_u \quad & e_T^2 + Ru_{pmp}^2, \\ \text{s.t.} \quad & \hat{T}_{a,out}^{int} \leq 80, \\ & \hat{T}_{c,pre}^{corr} \leq 50, \\ & \hat{T}_{c,out}^{inv} \leq 60, \\ & 0.1 \leq u_{pmp} \leq 1, \\ & 0.1 \leq u_{v1} \leq 1, \\ & 0 \leq u_{v2} \leq 1, \end{aligned} \quad (23)$$

where $u = [u_{pmp} \ u_{v1} \ u_{v2}]$ and R is a weighting constant. It should be noted that both u_{pmp} and u_{v1} are constrained to a minimum value of 0.1 as to ensure a certain coolant circulation through the compressor and DC-DC converter. The constrained optimization can be solved using the `fmincon` function from the optimization toolbox in Matlab. Since the dynamics associated with the thermal system are slow, this optimization can be triggered and solved every 10 seconds to yield a new set of solutions (u_{pmp} , u_{v1} and u_{v2}) to be used.

IV. RESULTS

The PI-control strategy and the OBC were tested under the 3 different scenarios shown in Table. I. The simulation results for those 3 scenarios are presented in Fig. 2. As shown in Fig. 2(a) for the PI-controller and Fig. 2(b) for the OBC, both control strategies were able to track the setpoints successfully for Scenario 1. It should be highlighted that, as is shown in Fig. 2(b) for the OBC, the constraint for $T_{c,in}^{DC}$ was struck which lead to a $T_{c,pre}$ lower than the maximum set to 50°C. This satisfies the control objectives set since the requirement for $T_{c,pre}$ is a constraint and not a setpoint to be tracked.

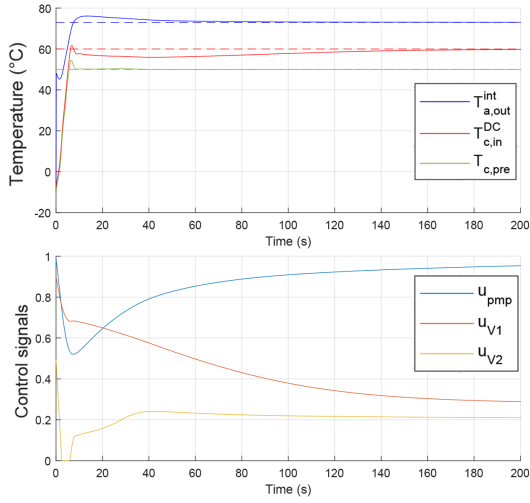
Despite of successful control in Scenario 1, when implementing the PI-control strategy, problems can still be encountered under certain conditions. This is due to the fact that, whenever a setpoint is reached, the respective actuator becomes stagnant and fixed which restricts the operation of the entire system. For example, since only $T_{a,out}^{int*}$ is used to control the pump, once this reference is reached, u_{pmp} remains constant. In the event where $u_{v2} = 1$ and $T_{c,pre} > T_{c,pre}^*$, the control strategy fails to provide more cooling and track $T_{c,pre}^*$. This is illustrated in Fig. 2(c) for Scenario 2. In an ideal case, the controller should be *smart* enough to increase u_{pmp} and manipulate u_{v2} such that the coolant flow through the radiator is increased. This would increase the heat dissipated \dot{Q}_{rad}

which in turns lowers $T_{c,pre}$ to a point where $T_{c,pre} \leq 55^\circ\text{C}$. To maintain the same temperature where $T_{a,out}^{int} = T_{a,out}^{int*}$, the *smart* controller would then reduce the coolant flow through the intercooler via changing u_{v1} . In Fig. 2(e), Scenario 3 with PI-control is illustrated. It can be seen that a problem, similar to the problem depicted in Scenario 2, is encountered. The distinction here is that, in Scenario 2, the control of $T_{a,out}^{int}$ is successful and u_{pmp} remains constant while u_{v1} and u_{v2} both saturate and lose control of the coolant temperatures. In Scenario 3, however, the coolant temperatures are successfully controlled meaning that both u_{v1} and u_{v2} remain constant. Under this constricted range of operation, u_{pmp} saturates and fails to control $T_{a,out}^{int}$. Controller saturation was, however, not encountered with the OBC as seen in Fig. 2(d) and Fig. 2(f). All control objectives were successfully fulfilled by the OBC for Scenario 2 and Scenario 3. This demonstrates a clear advantage of implementing the OBC instead of the PI-control strategy.

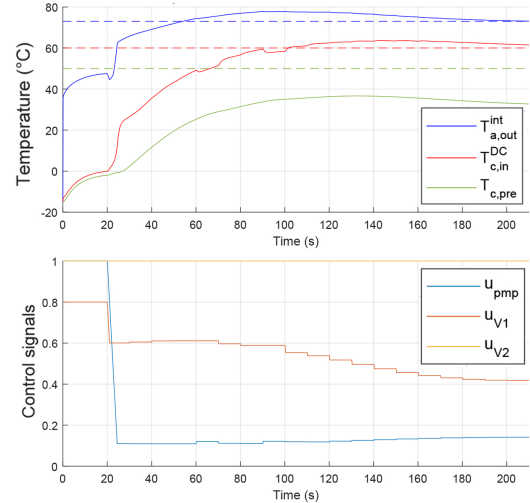
A drawback of using PI-controllers for the FCAC is the inefficiency associated with the pump operation. This is demonstrated in Fig. 2(a) for Scenario 1. There are namely two ways of increasing the cooling effect of the radiator \dot{Q}_{rad} : either by increasing the mass flow delivered by the pump or diverting more mass flow through the radiator using valve V-2. While V-2 does not consume energy at steady state, the pump consumes energy based on the coolant flow rate. Accordingly, a more optimal solution to decreasing $T_{c,pre}$ is to increase u_{v2} and then increase u_{pmp} once u_{v2} is saturated at 1. However, it can be seen that $u_{v2} = 0.29$ at steady state for Scenario 1. For more efficient operation, u_{v2} should be increased while u_{pmp} should be decreased to reduce the power consumption of the pump. This was seen with the OBC as shown in Fig. 2(b). The pump control action was less with the OBC ($u_{pmp} = 0.14$) than with the PI-control strategy ($u_{pmp} = 0.95$).

Another issue of using PI-controllers is that, while $T_{c,in}^{dc}$ must remain smaller than 62°C and $T_{c,pre}$ less than 55°C, these are not setpoints; rather, they are constraints. With the PI-controllers, the system operation is restricted to $T_{c,in}^{dc} = T_{c,in}^{dc*}$ and $T_{c,pre} = T_{c,pre}^*$ which does not ensures optimal operation of the system. In certain scenarios, this may be either inefficient or even infeasible. The temperature limitations on $T_{c,pre}$ and $T_{c,in}^{dc}$ are, however, intrinsically considered by the OBC. Accordingly, the OBC is not limited to operate in the range where $T_{c,in}^{dc} = T_{c,in}^{dc*}$ and $T_{c,pre} = T_{c,pre}^*$ and can therefore better avoid controller saturation. Moreover, since the cost function of the optimization problem, shown in (23), was designed to minimize u_{pmp} , the OBC leads to lower power consumption than the PI-control strategy.

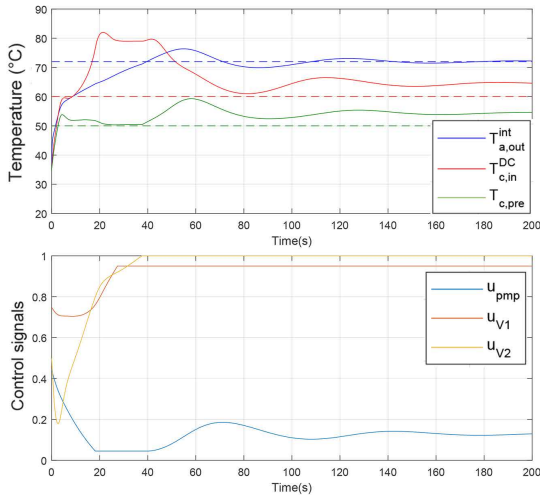
Table. II presents the steady-state values of the control inputs and of the outputs for both the PI-control strategy and the OBC. When comparing the two, it can be seen that in Scenario 1, both were able to fulfill the three crucial control objectives. From a steady-state point of view, in Scenario 1, the constraints for both control strategies were satisfied. Nevertheless, while at steady state $u_{pmp} = 0.95$ for the PI-controller, the OBC lead to a much lower pump power consumption with $u_{pmp} = 0.14$. The high pump power consumption was highlighted grey for emphasis. The high power consumption



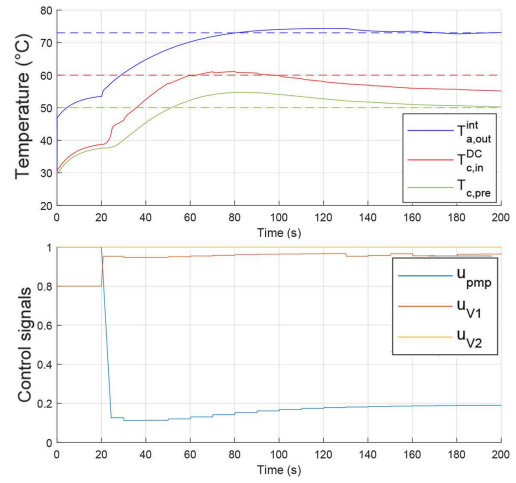
(a) Scenario 1 using PI-control



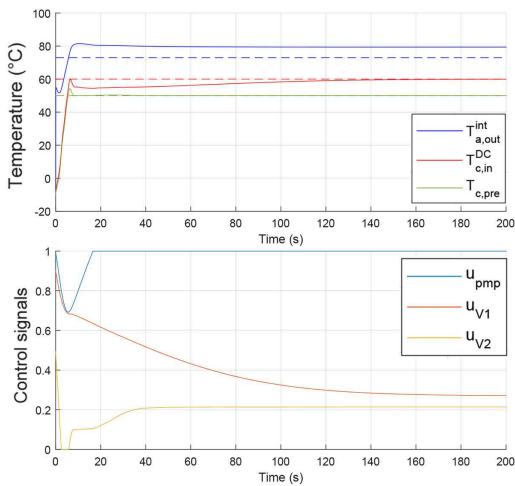
(b) Scenario 1 using OBC



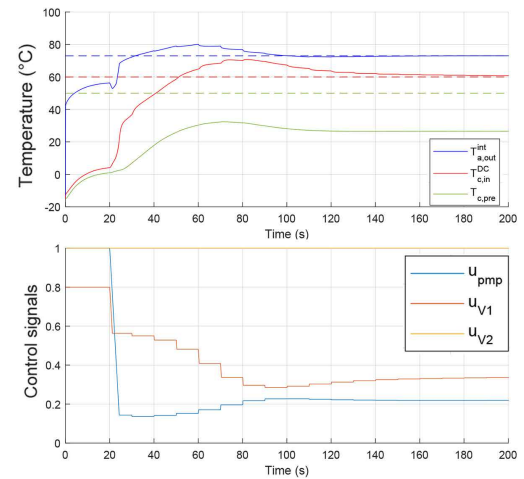
(c) Scenario 2 using PI-control



(d) Scenario 2 using OBC



(e) Scenario 3 using PI-control



(f) Scenario 3 using OBC

Fig. 2. Simulation results

TABLE II
SIMULATION RESULTS OF PI-CONTROL AND OBC (STEADY-STATE VALUES)

	u_{pmp}		u_{v1}		u_{v2}		$T_{a,out}^{int}$ (°C)		$T_{c,in}^{DC}$ (°C)		$T_{c,pre}$ (°C)		Pump Power (W)	
	PI	OBC	PI	OBC	PI	OBC	PI	OBC	PI	OBC	PI	OBC	PI	OBC
Scenario 1	0.95	0.14	0.29	0.41	0.21	1.00	72	72	60	60	50	32	902	20
Scenario 2	0.33	0.19	0.90	0.93	1.00	1.00	72	72	66	55	59	50	108	36
Scenario 3	1.00	0.22	0.28	0.32	0.21	1.00	80	72	60	60	50	27	1000	48

resulting from PI-control was also seen in Scenario 3 with $u_{pmp} = 1$ (*saturated*) and $u_{pmp} = 0.14$ for the OBC. This demonstrates a clear advantage of opting for the OBC rather than the PI-control strategy. For a fuel cell vehicle, using an OBC would lead to an increase in system efficiency due to the reduction of parasitic consumption. When examining Scenarios 2 and 3 for both controllers, it can be clearly seen that the PI-control strategy fails to satisfy the constraints, as indicated with the red highlighting, due to the cross coupling discussed in Section III-A. When tested with the OBC, it can be seen that this issue is completely resolved. While the PI-control strategy may seem more attractive due to its relatively simple nature, it may fail to satisfy constraints and cannot guarantee efficient operation of the FCAC. This remains the case regardless of how the PI parameters are tuned.

V. IMPLEMENTATION ON AUTOMOTIVE MICROCONTROLLER

Implementing the developed OBC strategy requires a solver for the optimization problem. This makes its implementation more challenging. Nevertheless, the structure of the OBC can be further simplified for series production implementation without the need of a solver. This is possible to the convexity of the optimization problem and can be done using the proposed SSO. The following control logic, for example, guarantees that the constraints are satisfied and that the power consumption of by the pump is kept to a minimum given that the radiator is sufficiently large to provided the desired cooling power:

- 1) The initial condition for the optimization variables is set to be $u_{pmp} = 0.1$, $u_{v1} = 1$ and $u_{v2} = 1$. This ensures that the all of the coolant flows through the radiator and that intercooler is entirely bypassed. This set of control inputs can be used via the discussed SSO to evaluate the temperatures $\hat{T}_{a,out}^{int}$, $\hat{T}_{c,pre}^{corr}$ and $\hat{T}_{c,out}^{inv}$.
- 2) If at least one of the coolant temperature constraints for $\hat{T}_{c,pre}^{corr}$ and $\hat{T}_{c,out}^{inv}$ given in (23) is violated, u_{pmp} is increased by a defined increment Δu_{pmp} and the coolant temperatures are evaluated again. This is repeated until both coolant temperature constraints are satisfied or $u_{pmp} = 1$.
- 3) If the evaluated $\hat{T}_{a,out}^{int}$ exceeds 73°C , u_{v1} is reduced by a defined increment Δu_{v1} towards a minimum of 0.1. This increases the coolant mass flow and the cooling power of the intercooler.
- 4) The air and coolant temperatures are evaluated using the SSO. If coolant temperature constraints are violated,

goto step 2). Otherwise, if $\hat{T}_{a,out}^{int}$ exceeds 73°C , go to step 3).

- 5) Steps 2) to 4) are repeated until all constraints are satisfied and either $\hat{T}_{a,out}^{int} < 73$ or $u_{pmp} = 1$.
- 6) Steps 1) to 5) are repeated every 10s. After each iteration, the control values after step 4) are applied and the SSO is updated with new values of $\hat{\alpha}_{int}$ and \hat{Q}_{corr} .

The control logic is well suited for the case where $T_{a,in}^{int} > 73^\circ\text{C}$ where the air requires cooling. In such cases, it more efficient to circulate the entire coolant flow through the radiator ($u_{v2} = 1$). The control logic can be further extended for the cases where $T_{a,in}^{int} < 73^\circ\text{C}$ such that the radiator is bypassed to use the heat generated in the other auxiliary components to warm up air entering the intercooler.

VI. CONCLUSIONS

In coupled systems with slow dynamics, such as vehicle-integrated thermal management systems, where the steady-state condition is of much more interest and relevance than the speed of the dynamic response, the proposed OBC strategy can be successfully utilized with reduced computational burden. This is a result of the using the control-oriented model based on a steady-state observer proposed in this paper. Using the SSO, knowledge of the dynamic behavior of each component is not needed. Therefore, the complexity of the optimization problem is significantly reduced making the approach more suitable for practical implementation. The innovative approach of implementing an OBC method on a VITM system was shown to lead to a reduction in the energy consumption of the main actuator (water pump) and resolve the coupling effect usually seen when using PI-based controllers. Furthermore, the use of the proposed OBC can be extended beyond VITMs. This can be done through first solving for the steady state given a certain set of control inputs and creating a SSO. The SSO can then be used as basis for the optimization problem.

ACKNOWLEDGMENTS

The work presented in this paper and all the associated tests done were conducted at Brose Fahrzeugteile GmbH & Co. This project has received funding from the Fuel Cells and Hydrogen 2 Joint Undertaking under grant agreement No 735969. This Joint Undertaking receives support from the European Union's Horizon 2020 research and innovation programme and Hydrogen Europe and N.ERGHY. The work is also an outcome of the Generalitat de Catalunya industrial doctorate program. The work of C. Ocampo- Martinez has

been partially supported by projects TED2021-129927B-I00 (MESHED) and PID2020-115905RB-C21 (L-BEST) funded by MCIN/ AEI /10.13039/5011000110033.

NOMENCLATURE

m	mass of fluid
u	internal energy
C_v, C_p	specific heat capacity under constant volume and pressure
h	enthalpy
W_{in}, W_{out}	inflow and outflow rates
\dot{Q}	heat flow rate
α	heat transfer coefficient
u_{pmp}	pump control action
T_{hot}, T_{cold}	temperatures at hot and cold volumes
$T_{c,pre}$	coolant temperature pre-cooling
u_{v1}, u_{v2}	control actions of valves V1 and V2
$a_{i,k}, b_{i,k}$	regression coefficients
e	error signal

Subscripts and Superscripts

$\hat{}$	estimated/observed value
*	reference value
\sim	correction signal
<i>corr</i>	corrected value
<i>in, out</i>	at inlet or at outlet
<i>a, c</i>	of air or of coolant
<i>int</i>	intercooler
<i>rad</i>	radiator
<i>dc</i>	DC-DC converter
<i>m</i>	compressor's motor
<i>inv</i>	compressor's inverter

REFERENCES

- [1] J. Larminie, A. Dicks, M. S. McDonald, Fuel Cell Systems Explained, Vol. 2, J. Wiley Chichester, UK, 2003.
- [2] R. M. Dell, P. T. Moseley, D. A. Rand, Towards Sustainable Road Transport, Academic Press, 2014.
- [3] A. C. Fernandes, E. A. Ticianelli, A Performance and Degradation Study of Nafion 212 Membrane for Proton Exchange Membrane Fuel Cells, Journal of Power Sources 193 (2) (2009) 547–554.
- [4] J. Lin, C. Lai, F. Ting, S. Chyou, K. Hsueh, Influence of Hot-pressing Temperature on the Performance of PEMFC and Catalytic Activity, Journal of applied electrochemistry 39 (7) (2009) 1067–1073.
- [5] S. G. Kandlikar, Z. Lu, Thermal Management Issues in a PEMFC Stack—A Brief Review of Current Status, Applied Thermal Engineering 29 (7) (2009) 1276–1280.
- [6] S. Cheng, C. Fang, L. Xu, J. Li, M. Ouyang, Model-based Temperature Regulation of a PEM Fuel Cell System on a City Bus, International Journal of Hydrogen Energy 40 (39) (2015) 13566–13575.
- [7] V. Liso, M. P. Nielsen, S. K. Kær, H. H. Mortensen, Thermal Modeling and Temperature Control of a PEM Fuel Cell System for Forklift Applications, international journal of hydrogen energy 39 (16) (2014) 8410–8420.
- [8] Y. Saygili, I. Eroglu, S. Kincal, Model Based Temperature Controller Development for Water Cooled PEM Fuel Cell Systems, International Journal of Hydrogen Energy 40 (1) (2015) 615–622.
- [9] J. T. Pukrushpan, A. G. Stefanopoulou, H. Peng, Control of Fuel Cell Power Systems: Principles, Modeling, Analysis and Feedback Design, Springer Science & Business Media, 2004.
- [10] L. Xing, W. Xiang, R. Zhu, Z. Tu, Modeling and thermal management of proton exchange membrane fuel cell for fuel cell/battery hybrid automotive vehicle, International Journal of Hydrogen Energy 47 (11) (2021). doi:10.1016/j.ijhydene.2021.10.146.
- [11] A. P. Vega-Leal, F. R. Palomo, F. Barragán, C. García, J. J. Brey, Design of Control Systems for Portable PEM Fuel Cells, Journal of power sources 169 (1) (2007) 194–197.
- [12] T. Hasegawa, H. Imanishi, M. Nada, Y. Ikogi, Development of the Fuel Cell System in the Mirai FCV, Tech. rep., SAE Technical Paper (2016).
- [13] J. Xu, C. Zhang, R. Fan, H. Bao, Y. Wang, S. Huang, C. S. Chin, C. Li, Modelling and Control of Vehicle Integrated Thermal Management System of PEM Fuel Cell Vehicle, Energy 199 (2020) 117495.
- [14] J. Xu, C. Zhang, Z. Wan, X. Chen, S. H. Chan, Z. Tu, Progress and perspectives of integrated thermal management systems in pem fuel cell vehicles: A review, Renewable and Sustainable Energy Reviews 155 (2022) 111908.
- [15] D. Watzenig, Comprehensive Energy Management-Safe Adaptation, Predictive Control and Thermal Management, Springer, 2018.
- [16] Y. Wang, J. Li, Q. Tao, M. H. Bargal, M. Yu, X. Yuan, C. Su, Thermal management system modeling and simulation of a full-powered fuel cell vehicle, Journal of Energy Resources Technology 142 (6) (2020).
- [17] J. Lescot, A. Sciarretta, Y. Chamaillard, A. Charlet, On the integration of Optimal Energy Management and Thermal Management of Hybrid Electric Vehicles, in: 2010 IEEE Vehicle Power and Propulsion Conference, IEEE, 2010, pp. 1–6.
- [18] G. Ao, J. Qiang, H. Zhong, X. Mao, L. Yang, B. Zhuo, Fuel Economy and NOx Emission Potential Investigation and Trade-off of a Hybrid Electric Vehicle Based on Dynamic Programming, Proceedings of the Institution of Mechanical Engineers, Part D: Journal of Automobile Engineering 222 (10) (2008) 1851–1864.
- [19] G. Rousseau, D. Sinoquet, P. Rouchon, Constrained Optimization of Energy Management for a Mild-hybrid Vehicle, Oil & Gas Science and Technology-Revue de l'IFP 62 (4) (2007) 623–634.
- [20] A. Sciarretta, L. Guzzella, Control of Hybrid Electric Vehicles, IEEE Control Systems Magazine 27 (2) (2007) 60–70.
- [21] J. Lopez-Sanz, C. Ocampo-Martinez, J. Alvarez-Florez, M. Moreno-Eguilaz, R. Ruiz-Mansilla, J. Kalmus, M. Gräeber, G. Lux, Nonlinear Model Predictive Control for Thermal Management in Plug-in Hybrid Electric Vehicles, IEEE Transactions on Vehicular Technology 66 (5) (2016) 3632–3644.
- [22] J. H. Lee, K. Ramamurthi, Fundamentals of Thermodynamics, CRC Press, 1998.



Yousif Eldigair received the B.S. in electrical engineering from The Petroleum Institute, Abu Dhabi, United Arab Emirates in 2013 and the M.Sc. in electrical engineering from Khalifa University, Abu Dhabi, United Arab Emirates in 2015. He is currently pursuing a Ph.D. degree in automatic control from the Universitat Politècnica de Catalunya - BarcelonaTech (UPC), Barcelona, Spain. In 2017, he was accepted into an industrial doctoral program offered as part of a collaboration between Brose Fahrzeugteile, Würzburg, Germany and the Universitat Politècnica de Catalunya - BarcelonaTech (UPC). The doctoral program lies within the framework the European-funded INN-Balance project. The project is aimed at the development of automotive fuel cell systems. In 2021, he was appointed by Brose as a Software Developer to design control systems for automotive R&D projects. His research interests revolve around the control of electric drives, automotive hydrogen fuel cell systems and thermal management systems.



Cristian Kunusch (S'03-M'10-SM'16) received the B.S., M.Sc., and Ph.D. degrees in electronic engineering from the National University of La Plata, Buenos Aires, Argentina, in 2003, 2006, and 2009, respectively. In 2010, he was appointed as a Post-doctoral Fellow of the Spanish National Research Council, Institut de Robòtica i Informàtica Industrial, Barcelona, Spain. Between 2011 and 2013, he ran a Marie Curie project funded by the European Commission. In 2014, he joined the Electric Drives Advanced Development team of Brose

Fahrzeugteile, Würzburg, Germany, as a Senior Researcher and R&D Project Manager. Since 2019 he is working as Lead System Architect for e-Axles at Valeo-Siemens eAutomotive. His main research interests include variable structure systems and their applications to the control and observation of fuel-cell-based systems and eAxles in automotive applications.



Carlos Ocampo-Martinez (S'97-M'11-SM'13) received the electronic engineering degree and the M.Sc. degree in industrial automation from the Universidad Nacional de Colombia, Manizales campus, in 2001 and 2003, respectively, and the Ph.D. degree in control engineering from the Universitat Politècnica de Catalunya - BarcelonaTech (UPC), Barcelona, Spain. After a year as postdoctoral fellow of the ARC Centre of Complex Dynamic Systems and Control (University of Newcastle, Australia) working on fault-tolerant control of linear dynamic

systems, he was with the Spanish National Research Council (CSIC) at the Institut de Robòtica i Informàtica Industrial (IRI) in Barcelona as a Juan de la Cierva research fellow working on partitioning and hierarchical decentralized control of large-scale complex flow networks. Since 2011, he is with the UPC, Automatic Control Department (ESAI), currently as an associate professor in automatic control and model predictive control. From 2014 until 2018, he was Deputy Director of the Institut de Robòtica i Informàtica Industrial (CSIC-UPC). He has published over two hundred of scientific papers related to automatic control and dynamic systems and has authored the book entitled Model Predictive Control of Wastewater Systems and co-edited the books entitled Transport of Water Versus Transport Over Water and Real-Time Monitoring and Operational Control of Drinking Water Systems, all of these books with Springer. His main research interests include constrained model predictive control, large-scale systems management (partitioning and noncentralized control), and industrial applications (mainly related to the key scopes of water, energy, and smart manufacturing under IoT framework). He belongs to the Conference Editorial Board of the IEEE CSS.